CHAPTER 118

REFLECTION COEFFICIENTS OF THE STEP-SHAPED SLIT CAISSON ON THE RUBBLE MOUND

Sung Mo. Ahn,[1] Ryuichi Fujiwara[2], Hiroshi Matsunaga[3], Katsuhiko Kurata[4], Shohachi Kakuno[5]

ABSTRACT

The characteristics of the reflection coefficients of a step-shaped slit caisson on the rubble mound are examined by experimental data.A numerical analysis which combines the method of matched asymptotic expansions with a boundary element method has been applied for the calculation of the reflection coefficients of the caisson on the rubble mound. Numerical results are compared with experimental data to show the validity. Dimensions of the preferable cross-section of the step-shaped slit caisson on the rubble mound are discussed and obtained through the numerical results.

1. INTRODUCTION

Many kinds of perforated breakwaters, seawalls, and quay-walls have been constructed in Japan. A large number of studies about the hydraulic cahracteristics of this type of breakwaters have been performed since Jarlan's original work (1961). Reflection coefficients of the structures of this type depend strongly on the relative wave chamber width, the ratio of the wave chamber width to the wave length, and low reflection coefficient can be expected only in a narrow band of wave frequency. From this reason, a new type of breakwater with a step-shaped slit wall, whose cross section is shown schematically in **Fig. 3**, has been developed recently and some very fascinating

---

1 Research Engineer, Hydraulic Engineering Laboratory,Technical Research Institute , Toyo Const. Co. Ltd. 3-7-16, Naruo -hama , Nishinomiya, Hyogo, Japan
2 Senior Research Engineer, ditto
3 Senior Engineer, Osaka Branch,Toyo Const.Co. Ltd.
4 General Manager, Technical Research Institute Toyo Const. Co. Ltd.
5 Assoc. Prof., Dept. of Civil Engrg.,Osaka City Univ.3-3-138,Sugimoto,Sumiyoshiku, Osaka,Japan

results have been found. It was found that this breakwater has low reflection in a wider range of wave frequency compared to conventional slit-type breakwaters. Although a numerical analysis which combines the method of matched asymptotic expansions with a boundary element method(BEM) has successfully been applied for calculation of the reflection coefficients of this structure(Kakuno et al., 1989), the previous analysis was on the condition of non rubble mound. It is essential to verify the effect of rubble mound and to discuss the preferable shape of the *step-shaped slit caisson(SSC)* on the rubble mound for the objective of the construction of this breakwater in the field.

The main objective of the present study is to present the preferable shape and dimensions of the *SSC* on the rubble mound from the viewpoint of the reflection coefficient.Wave flume experiments were carried out for this objective and the results were compared with those of a modified numerical model which was modified to take the effect of the rubble mound into consideration.

2 NUMERICAL ANALYSIS

2-1 Assumptions and the Boundary Conditions

We consider two-dimensional problem as shown in **Fig.1**. Assuming non-viscous and incompressible fluid except the region of the vicinity of the slits, we may have the velocity potencial for the fluid motion in the whole fluid domain Ω. The velocity potential $\phi(x,z)$, which excludes the time term $\exp(-i\sigma t)$ satisfies the governing equation and the boundary conditions as follows :

$$\nabla^2\phi = 0 \qquad ;in \quad \Omega \tag{1}$$

$$\partial\phi/\partial y - \nu\phi = 0 \qquad ;on \quad y = 0 \tag{2}$$

$$\partial\phi/\partial y = 0 \qquad ;on \quad y = -h \tag{3}$$

$$\partial\phi/\partial n = 0 \qquad ;on \quad S_U \tag{4}$$

$$\partial\phi/\partial x = 0 \qquad ;on \quad x = l \tag{5}$$

$$\lim_{|x| \to \infty} \left(\partial\phi_{sc}/\partial|x| - ik\phi_{sc}\right) = 0 \qquad ;x \to -\infty \tag{6}$$

Radiation condition, Eq.(6), can be rewritten for this problem with a complex reflection coefficient ρ as follows:

$$\phi(x,y)\big|_{x \to -\infty} \to \left(e^{ikx} + \rho e^{-ikx}\right)\cosh k(y+h)/\cosh kh \tag{7}$$

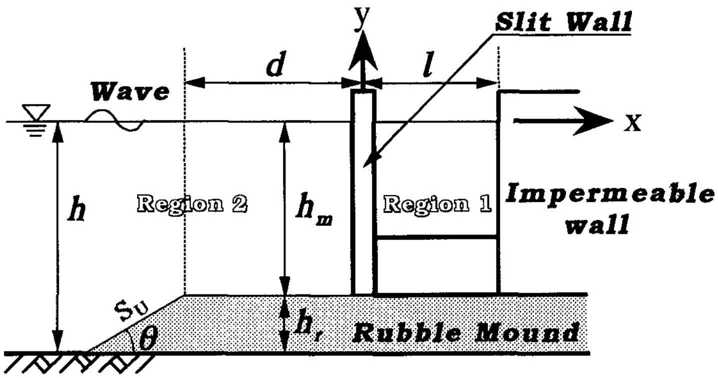

Figure 1. Definition sketch

2-2 A Method of Matched Asymptotic Expansions

(1) Far-field Solutions

The flow domain is devided into two fields; one is the region 1 and the other the region 2 as shown in **Fig. 1**. Applying Green's theorem to the governing equation in each region, far-field solutions having no local influence by slit walls are derived as follows:

$$\phi_1(\xi,\eta) = \int_{-h_m}^{0}\left[\frac{\partial\phi_1}{\partial x}(0_+,y)G_1(0_+,y;\xi,\eta) - \phi_1(0_+,y)\frac{\partial G_1}{\partial x}(0_+,y;\xi,\eta)\right]dy$$

$$+\int_{-h_m}^{0}\phi_1(l,y)\frac{\partial G_1}{\partial x}(l,y;\xi,\eta)dy \quad (8)$$

$$\phi_2(\xi,\eta) = \phi_0(\xi,\eta)$$

$$+\int_{-h_m}^{0}\left[\phi_2(0_-,y)\frac{\partial G_2}{\partial x}(0_-,y;\xi,\eta) - \frac{\partial\phi_2}{\partial x}(0_-,y)G_2(0_-,y;\xi,\eta)\right]dy$$

$$+\int_{-d}^{0}\phi_2(x,-h_m)\frac{\partial G_2}{\partial y}(x,-h_m;\xi,\eta)dx + \int_{\Gamma}\phi_2(x,y)\frac{\partial G_2}{\partial n}(x,y;\xi,\eta)ds \quad (9)$$

where G_1 and G_2 are Green's functions, (ξ,η) is a coordinates in the fluid domain, (x,y) is a coordinates on the pass of integration, Γ is the pass of integration on the slope of the rubble mound, $\phi_2(x,y)$ is the velocity potential on the Γ, and $\phi_2(x,-h_m)$ is the velocity potential on the flat top of the rubble mound. $\phi_0(\xi,\eta)$ is the velocity potential of the incident waves which may be written as:

$$\phi_0(\xi,\eta) = \exp(ik\xi)\cosh k(\eta+h)/\cosh kh \tag{10}$$

(2) Near-field Solutions

The near-field solutions which must satisfy the boundary condition on the surfaces of cylinders may be taken as an oscillating flow through the slits between cylinders with a velocity amplitude $U(\eta)$

$$\phi(\xi,\eta) = (\xi \pm C(\eta))U(\eta) + C_0'(\eta) \tag{11}$$

where the positive and negative signs correspond to region 1 and region 2, respectively, $C_0'(\eta)$ is a complex constant, and $C(\eta)$ is a complex blockage coefficient (Kakuno et al., 1993) whose real part corresponds to the coefficient of the inertia resistance and imaginary part to the coefficient of energy dissipation due to the separation at slits.

(3) Matching and reflection coefficient of the *SSC*

In order to match the inner expansions of the far-field solutions and the outer expansions of the near-field solutions, we have to obtain the limit form for $\xi \to \pm 0$ in Eq.(8) and Eq.(9):

$$\begin{aligned}\phi_1(0_+,\eta) = {} & 2\int_{-h_m}^{0} \frac{\partial\phi_1}{\partial x}(0_+,y)G_1(0_+,y;0_+,\eta)dy \\ & + 2\int_{-h_m}^{0} \phi_1(l,y)\frac{\partial G_1}{\partial x}(l,y;0_+,\eta)dy\end{aligned} \tag{12}$$

$$\begin{aligned}\phi_2(0_-,\eta) = {} & 2\phi_0(0_-,\eta) - 2\int_{-h_m}^{0} \frac{\partial\phi_2}{\partial x}(0_-,y)G_2(0_-,y;0_-,\eta)dy \\ & + 2\int_{-d}^{0} \phi_2(x_1,-h_m)\frac{\partial G_2}{\partial y}(x,-h_m;0_-,\eta)dx \\ & + 2\int_{\Gamma} \phi_2(x,y)\frac{\partial G_2}{\partial n}(x,y;0_-,\eta)ds\end{aligned} \tag{13}$$

Equation (12) and (13) may be matched with Eq.(11) to yield unknown parameters, $U(\eta)$, $\phi(x,y)$ and $\phi_2(x,y)$ and we may have:

$$\begin{aligned} C(\eta)U(\eta) + \phi_0(0_-,\eta) = {} & \int_{-h_m}^{0} U(y)\bullet\left[G_1(0_+,y;0_+,\eta) + G_2(0_-,y;0_-,\eta)\right]dy \\ & + \int_{-h_m}^{0} \phi_1(l,y)\frac{\partial G_1}{\partial x}(l,y;0_+,\eta)ds - \int_{-d}^{0} \phi_2(x,-h_m)\frac{\partial G_2}{\partial y}(x,-h_m;0_-,\eta)dx \\ & - \int_{\Gamma} \phi_2(x,y)\frac{\partial G_2}{\partial n}(x,y;0_-,\eta)ds\end{aligned} \tag{14}$$

Also we may derive three equations as the limit form of Eqs. (8) and (9) making (ξ,η) approach impermeable surfaces:

$$\phi_1(l,\eta) = 2\int_{-h_m}^{0}\left[\frac{\partial\phi}{\partial x}(0+,y)G_1(0+,y;l,\eta) - \phi_1(0+,y)\frac{\partial G_1}{\partial x}(0+,y;l,\eta)\right]dy \qquad (15)$$

$$\phi_2(\xi,-h_m) - \int_{-d}^{0}\phi_2(x,-h_m)\frac{\partial G_2}{\partial y}(x,-h_m;\xi,-h_m)dx = \phi_0(\xi,-h_m)$$

$$+\int_{-h_m}^{0}\left[\phi_2(0-,y)\frac{\partial G_2}{\partial x}(0-,y;\xi,-h_m) - \frac{\partial\phi_2}{\partial x}(0-,y)G_2(0-,y;\xi,-h_m)\right]dy$$

$$+\int_{\Gamma}\phi_2(x,y)\frac{\partial G_2}{\partial n}(x,y;\xi,-h_m)ds \qquad (16)$$

$$\phi_2(\xi,\eta) - \int_{\Gamma}\phi_2(x,y)\frac{\partial G_2}{\partial n}(x,y;\xi,\eta)ds = \phi_0(\xi,\eta)$$

$$+\int_{-h_m}^{0}\left[\phi_2(0_-,y)\frac{\partial G_2}{\partial x}(0_-,y;\xi,\eta) - \frac{\partial\phi_2}{\partial x}(0_-,y)G_2(0_-,y;\xi,\eta)\right]dy$$

$$+\int_{-d}^{0}\phi_2(x,-h_m)\frac{\partial G_2}{\partial y}(x,-h_m;\xi,\eta)dx + \int_{\Gamma}\phi_2(x,y)\frac{\partial G_2}{\partial n}(x,y;\xi,\eta)ds \qquad (17)$$

Obtaining $U(\eta), \phi_1(l,y), \phi_2(x,-h_m), \phi_2(x,y)$ from Eqs.(14) through (17), we may calculate limit values for Eq.(8) and (9) . Comparing these limit values with Eq.(7), the reflection coefficient can be obtained.The numerical method for the type of those equations has been discussed in detail, for example, by Macaskill(1979).

3 EXPERIMENTS

A wave flume in which model tests were conducted is *40m* long, *1.0m* wide and *2.0m* deep, and is shown in **Fig. 2**.The slope of the foreshore was uniform with 1:100. The cross section of the breakerwater model is shown in **Fig.3**,where the water depth on the horizontal bottom was kept constant: $h = 50cm$. To examine the characteristics of the reflection coefficient and to verify the validity of the calculation, we used *12* types of model caissons with *2*types of rubble mound. The test conditions are shown in **Table 1**. From measured wave profiles in front of the caisson, the reflected wave height and the reflection coefficients were estimated by using Goda's method (Goda et al.,1976).

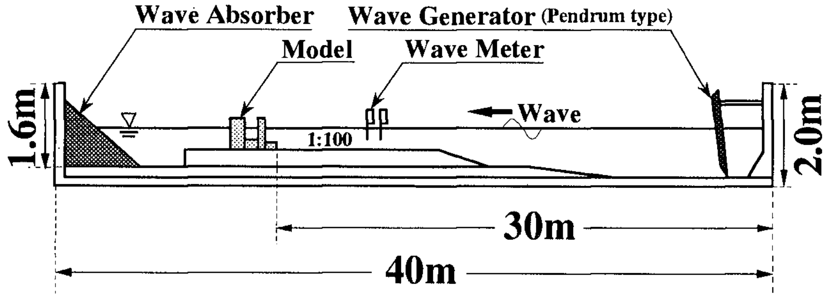

Figure 2. Wave Flume

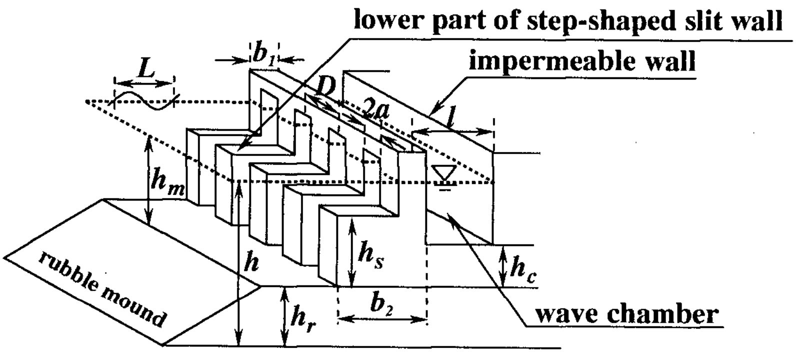

Figure 3. Cross Section of Breakwater

Table 1. Test Condition

Water Depth (h)	50 *cm*
Height of Rubble Mound (h_r)	h_r / h =0.14 , 0.33 (2 Types)
Wave Period(T)	0.73～2.19 sec (6 Types)
Wave Height(H)	H / L = 0.01 , 0.02 (2 Types)
Model Breakwater	12 Types

4 DISCUSSION

4-1 Results of Experiments

In **Fig. 4**, the variation of the reflection coefficients as a function of the relative wave chamber width, l/L, is presented with a parameter h_s/h_m, where h_s is the height of the lower part of the slit wall and h_m the depth of the top of the rubble mound. From **Fig. 4**, it is observed that the reflection coefficients K_R become slightly smaller at larger period as h_s/h_m becomes large, that is, the height of the lower part of the slit wall(h_s) increases. **Fig. 5** shows the variation of the reflection coefficients as functions of the relative wave chamber width and a parameter h_c/h_m, where h_c is the height of the bottom of the wave chamber. From the figure, it is obvious that the reflection coefficients K_R become smaller at longer period as the height of the bottom of the wave chamber becomes large.However,in the shorter period the reflection coefficients become large with increasing h_c/h_m .Also, the value of l/L where the reflection coefficient attains minimum value becomes small.These results implies wave energy must be dissipated effectively by raising the bottom of the wave chamber; that is, the flow through the gaps of the lower part of slit wall is directed upward and is merged with the flow through the gap of the upper part of slit wall.Therefore, the flow through the gap of slit wall is accelerated and more energy loss due to eddy-formation and flow separation may be expected.From these results, lower part of the slit wall and raised bottom of the wave chamber may be effective for the reduction of the reflection coefficient.**Fig. 6** and **Fig. 7** show the reflection coefficients as functions of the relative wave chamber length and h_r/h (**Fig.6**), where h_r is the height of the rubble mound, or the wave steepness, H/L (**Fig.7**). From these figures, as h_r/h increases from 0.14 to 0.33, or as the wave steepness increases, the reflection coefficients K_R become small.

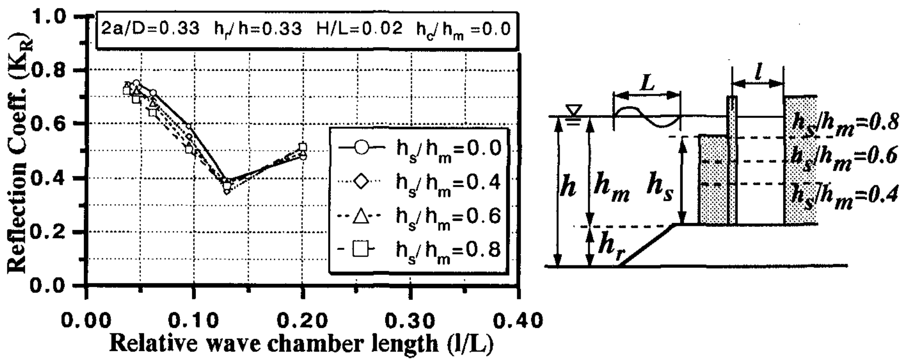

Figure 4. Effect of the height of the lower part of slit wall

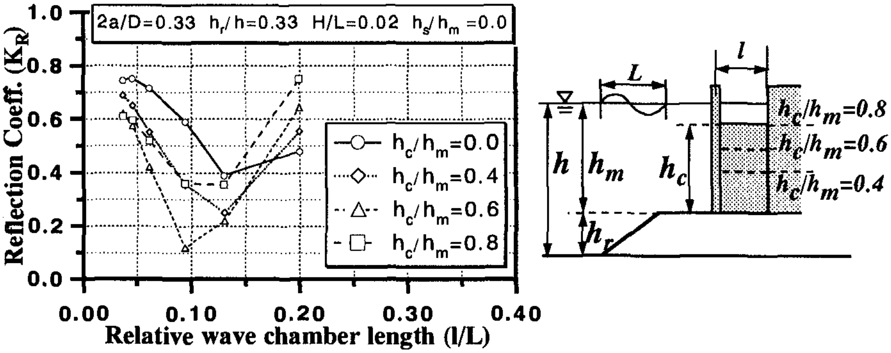

Figure 5. Effect of the depth of the wave chamber

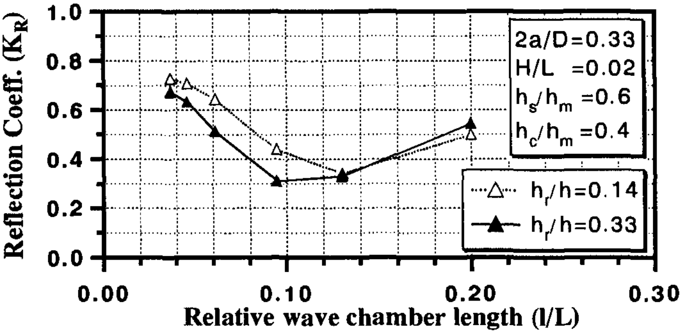

Figure 6. Effect of the height of rubble mound

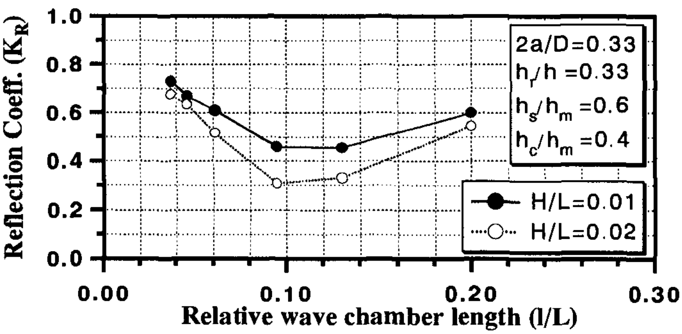

Figure 7. Effect of the wave steepness

4-2 Comparison of Numerical and Experimental Results

In **Fig. 8**, an example of the comparison of numerical results and experimental data for the reflection coefficients is shown. From **Fig. 8**,it is obvious that the numerical results of the reflection coefficients agree well with the experimental ones and the validity of the present numerical scheme is shown.

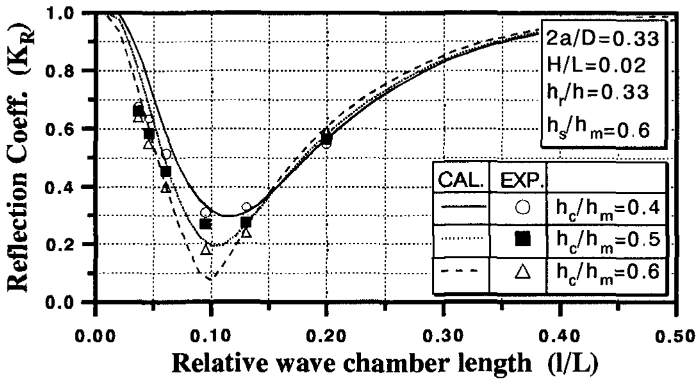

Figure 8. Comparison of numerical and experimental reflection coefficient

4-3 Preferable Shape and Dimension of the *SSC* on the Rubble Mound

The preferable shape and dimensions of the ***SSC*** are discussed on the basis of the criteria as follows:

1) ***for short-period waves***, *the value of the reflection coefficient is almost the same as one of the conventional slit-type caisson.*
2) ***for long-period waves***, *the value of the reflection coefficient is smaller than the conventional slit-caisson in a wider range of wave period.*

Fig.9 shows the relation between the reflection coefficients K_R and the relative wave chamber width, l/L, with a parameter h_s/h_m, of the ***SSC*** on the rubble mound and the conventional slit-type caisson. As the height of the lower part of the slit wall increases, the minimun value of K_R shifts to longer period slightly. In order to decide the preferable dimension of the *SSC* , the criteria as mentioned above was applied in the range of the relative wave chamber width where the reflection coefficients become smaller than 0.5. **Table 2** shows the range of the relative wave chamber width for $K_R \le 0.5$ read from **Fig. 9**. From **Table 2**, the preferable height of lower part of the slit wall ,h_s, should be taken as 0.6 times the depth of the top of the rubble mound,h_m. The same routine may be performed for the preferable depth of the wave chamber, and the results of that are shown in **Fig.10** and **Table 3**. From **Table 3**, the preferable height of the raised bottom of the wave chamber ,h_c, may be judged to be 0.4 times the depth of the top of the rubble mound,h_m. Therefore, dimensions of the most preferable cross-section of the *SSC* is a combination of,$h_s = 0.6h_m$ and $h_c = 0.4h_m$. Now, as readily expected, the gap-ratio $2a/D$, where $2a$ is the gap,or slit,width and D is the distance between adjacent cylinders, is very effective parameter on the reflection coefficients of this type of structure. **Fig. 11** shows the effect of the gap-ratio $2a/D$ for the cross section of the *SSC* with $h_s = 0.6h_m$ and $h_c = 0.4h_m$. **Table 4** shows that the most preferable gap-ratio $2a/D$ of the *SSC* is 0.25.

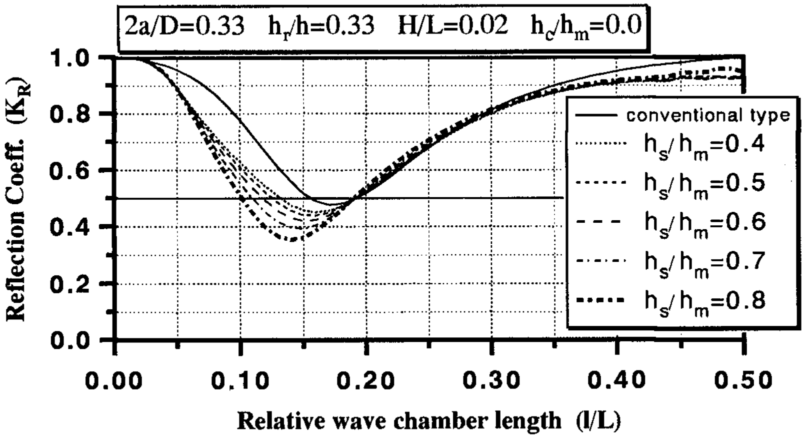

Figure 9. Preferable height of the lower part of the slit wall

Table 2. Range of relative wave chamber length l/L

h_s/h_m	the range of l/L with $K_R \le 0.5$
Conventional type	0. 15~0.19
0.2	0.14~0.19
0.3	0.13~0.19
0.4	0.12~0.19
0.5	0.11~0.18
0.6	0.10~0.18

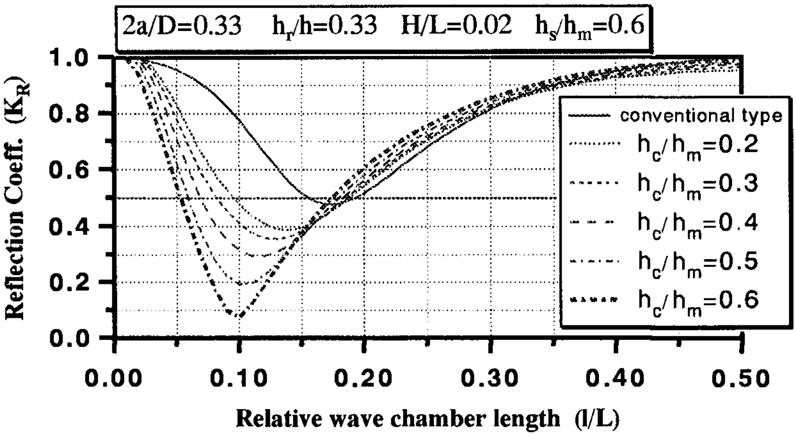

Figure 10. Preferable depth of the wave chamber

Table 3. Range of relative wave chamber length l / L

h_c / h_m	the range of l / L with $K_R \leq 0.5$
Conventional type	0. 16~0.19
0.2	0.10~0.18
0.3	0.09~0.18
0.4	0.07~0.18
0.5	0.06~0.17
0.6	0.06~0.17

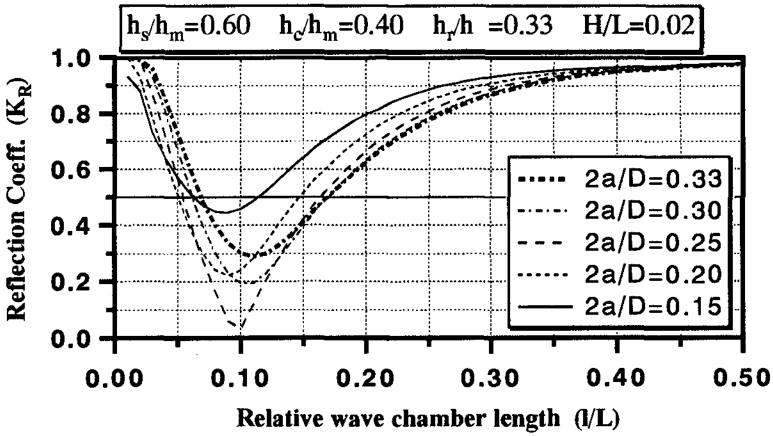

Figure11. Preferable gap ratio of the slit wall

Table 4. Range of relative wave chamber length l / L

$R_g (= 2a / D)$	the range of l / L with $K_R \leq 0.5$	minimum value of K_R
0.33	0.10~0.18	0.28
0.30	0.09~0.18	0.19
0.25	0.07~0.18	0.03
0.20	0.06~0.17	0.22
0.15	0.06~0.17	0.44

CONCLUSION

The main conclusions obtained from this study can be summarized as follows:.

1) Lower part of the slit wall and raised bottom of the wave chamber are effective for reduction of the reflection coefficient. The reflection coefficient of the *SSC* becomes low in a wider range of wave frequency than the conventional slit type caisson .

2) The numerical analysis which combines the method of the matched asymptotic expansion with BEM is supported and verified by the results of experiments on the reflection coefficients of the *SSC* on the rubble mound for regular waves.

3) Dimensions of the most preferable cross-section of the *SSC* is a combination of, the lower part of slit wall whose height is *60%* of the water depth of the top of the rubble mound and, the raised bottom of the wave chamber whose height is *40%* of the water depth of the top of the rubble mound, and the gap-ratio is *25%*.

The next step we should take is to examine the stability of the *SSC*, for the purpose of the construction of the *SSC* in deeper seas.

References

Fujiwara,R., T.Yosida.,K.Kurata.,S.Kakuno and K.Oda (1994) : A new type of breakwater with a Step-shaped slit wall ,*Int.Conf. on Hydro-Technical Engrg. for Port and Harbor Const.*, pp. 543-562.

Goda,Y.,Y.Suzuki (1976) : Estimation of incident and reflected waves in random wave experiments,*Proc.ICCE*, pp. 828-845.

Jarlan,G.E. (1961) : A perforated vertical wall breakwater,*The Doc & Harbour Authority, Vol. XLI,*No.486, pp. 394-398.

Kakuno,S.,K.Oda,T.Muramoto and T.Yosida (1986) : A concept of a complex blockage coefficient for evaluating energy loss effects at slit of structures ,*Proc.Japanese Conf. on Coastal Engrg*,Vol.33, pp. 407-411. (in Japanese)

Kakuno,S.,K.Oda,T.Fujita, S.Teraoka and T.Yosida (1989) : Wave behavior around slit-type structures with arbitrary vertical cross-sections ,*Proc. Japanese Conf. on Coastal Engrg*,Vol.36, pp. 499-503. (in Japanese)

Kakuno,S.,K.Oda, and P.L.-F.Liu (1993) : Scattering of water waves by vertical cylinders with a backwall ,*Proc.ASCE*, pp. 1258-1270.

Macaskill,C.(1979) : Reflection of water waves by a permeable barrier,*J.Fluid Mech.*,, Vol.95, pp. 141-157.